Received: 04 November 2024 | Revised: 16 January 2025 | Accepted: 30 March 2025

https://doi.org/10.56946/jce.v4i1.579

Journal of Chemistry and Environment

Research Article

Appraisal and Evaluation of Hydrogeochemical Processes in the Aquifer System of the South Eastern Coastal Area of Bangladesh

Nafisa Tamannaya Dina[1], Mohammad Zafrul Kabir[1*], Farah Deeba[1], Syed Hafizur Rahman[2], Md. Golam Rasul[1], Md. Ferdous Alam[3], Salma Sultana[3]

[1]Institute of Nuclear Minerals, Bangladesh Atomic Energy Commission, AERE, Savar, Dhaka-1349, Bangladeh.
[2]Department of Environmental Sciences, Jahangirnagar University, Savar, Dhaka-1342, Bangladesh.
[3]Institute of Nuclear Science and Technology, Bangladesh Atomic Energy Commission, AERE, Savar, Dhaka-1349, Bangladesh.

*Correspondence: zkabirbaec@gmail.com

Abstract

A hydrogeochemical study of groundwater in the aquifer system of the south eastern coastal area of Bangladesh was carried out to investigate the processes of groundwater hydrogeochemistry as well as the suitability of groundwater for drinking purposes. Water samples from tube wells (depths 6.5–165 m) were collected and examined for several water quality parameters to describe the hydrogeochemical characteristics. Most of the water samples were found to be fresh and soft water with few numbers of hard and brackish water. The overall sequence of cation and anion throughout the study area is Ca^{2+}> Na^{+}> Mg^{2+}> K^{+} and HCO_3^- > CO_3^- > NO_3^- > SO_4^{2-}> Cl^- respectively. Maximum water quality parameters satisfy the drinking water quality standard proposed by WHO. The piper diagram suggests that Ca^{2+}-Mg^{2+}-HCO_3^- (80%) and Ca^{2+}-Na^{+}-HCO_3^- (20%) facies are the predominant water types. Gibb's plot implies a rock-dominant inheritance that regulates the groundwater chemistry. The most significant hydrogeochemical processes in the study area are carbonate weathering. Correlation analysis recommends that TDS, EC, Na^{+}, Ca^{2+}, Cl^-, and SO_4^{2-} are strongly correlated with each other, indicating their contribution to water mineralization. The principal component analysis (PCA) and cluster analysis show that weathering and leaching of parent rocks are the leading environmental sources that influence the groundwater hydrochemistry.

.**Keywords:** Coastal aquifer, Hydrogeochemistry, Hydrochemical classification, Rock water interaction

1. Introduction

Groundwater is assumed to be a valuable and significant freshwater resource that plays an essential role in human existence and the sustained operation of our planetary ecology, particularly in areas containing few freshwater bodies, such as coastal regions [1-4]. Numerous natural and anthropogenic variables influence water's physical, chemical, and biological characteristics and control the water quality. Groundwater geochemistry is influenced by factors like geology, the extent of chemical weathering of different parent rocks, aquifer characteristics, and rock-water interaction [5-7]. Groundwater travels from recharge to discharge zones, and the transient flow of water along void spaces and weathered zones as well as several hydrogeochemical mechanisms, change the chemical concentration of the water [8, 9]. Public health may be significantly impacted by the lack or high consumption of those major, minor, and trace components in drinking water

[10]. To regulate and establish the quality of groundwater, its usage, as well as its management strategies, it is crucial to understand the geochemical processes that occur during groundwater flow. Additionally, various anthropogenic activities such as waste disposal facilities, industrial effluents, on-site sewage disposal, and agricultural runoff also influence the groundwater constituents [11-13]. The consequences of polluted groundwater on public health are often identified in various localities of Bangladesh. The structure and behavior of the aquifer systems can thus be thoroughly studied using hydrochemistry. In this instance, physico-chemical data was employed as a natural pathfinder to show how the hydrogeological system was structured and operated [14]. Many different factors affect the hydrochemistry of groundwater. Therefore, understanding hydrogeochemistry is necessary to ascertain the source of the chemical concentration of groundwater [15].

Cox's Bazar, the most populous and quickly expanding coastal city along the Bay of Bengal, is well-known for tourism because of its extraordinary environment and strategic location. The coastal groundwater reservoir serves as the most significant water source in the Cox's Bazar coastal area. Saltwater intrusion is the prime reason for coastal area groundwater contamination. As the consumption of fresh groundwater has risen over time, overharvesting of the aquifer, particularly in the dry season, causes abstractions. Besides this, heavy metal pollution and radioactive placer deposits, along with intense agricultural activities including excessive fertilizer and manure, impose a significant impact on the accessibility as well as the quality of water in this coastal aquifer. Therefore, this study describes the hydrochemistry of groundwater and establishes a correlation between the groundwater chemistry and the reservoir geology of the southeastern coastal area for the future sustainability of public health.

Various previous research studies evaluated the threat to human health from groundwater contamination by trace metals in Bangladesh coastal regions [16-19] as well as seawater intrusion at Cox's Bazar, Bangladesh [20-23]. Few researchers have tried to characterize the hydrochemical evaluation of the south-eastern coastal aquifer. The present research aimed to evaluate the hydrogeochemical processes that control groundwater chemistry in the coastal aquifer, illustrating major ion chemistry, hydrochemical facies, rock water interaction, and drinking water suitability.

2. Materials and methods

2.1. Study area

The present investigation was carried out at the south-eastern coastal area of Bangladesh located between 20°50′ to 21°20′ N and 91°55′ to 92°35′ E, extending from Cox's Bazar to Teknaf region (Fig. 1). This study area is previously described at [17]. This region comprises the foredune and backdune lying parallel to the current shoreline and south-eastern portion of hill ranges. The tropical rainfall causes roughly 3630 mm, rain annually from May to October. The mean annual temperature ranges from 26.7 °C to 32.2 °C (January to May). Geologically, this region is situated in the southern part of the Chittagong folded zone. Tectonically, when the late Cretaceous Indian plate separated from the main Gondwana land after that collided with the Eurasian plate in the north, the Burmese sub-plate in the west, forming the Bengal Basin and the Bay of Bengal [24]. From Cox's Bazar (north) to the Teknaf (south) region, the Eastern Coastal Zone is made up of a series of anticlines and synclines, comprising a distinct syncline in Cox's Bazar while an anticline in the Teknaf region [16, 25, 26]. The north-western portion of hill ranges, the foredune and the backdune bordered the studied area. The subsurface stratigraphy of the aquifer of foredunes and paleo-beach areas are formed of about (5 to 265 m) thick unconsolidated sedimentary strata of fine to medium sands with small patches of silty-clay and alluvium of Quaternary age [22]. Hydrogeologically, Bangladesh's coastal aquifer structure has been classified into three primary aquifer, and these aquifers are parted by leaky and discontinuous aquitards [16, 26]. Considering diverse soil characteristics based on the subsurface distribution of sediments identified by borehole lithology, continuous core drilling data, and resistivity survey data (vertical electrical sounding VES), the research area is

categorized into three principal aquifers—upper, middle, and lower. The upper unconfined aquifer (5 to 15 m depth) composed of fine to medium sand followed by the middle semi-confined aquifer (30 to 80 m depth) with same lithology. At a greater depth of more than 80 m, a lower confined aquifer consists of grey to dark grey fine to medium sand [23, 27].

Groundwater samples from local tube-wells of the study area were collected randomly based on different land use pattern considering population, industrial area and heavy placer mineral deposit area. Water samples are collected from the tube wells at depth varies from 6.5 to 37m i.e. upper and middle aquifer.

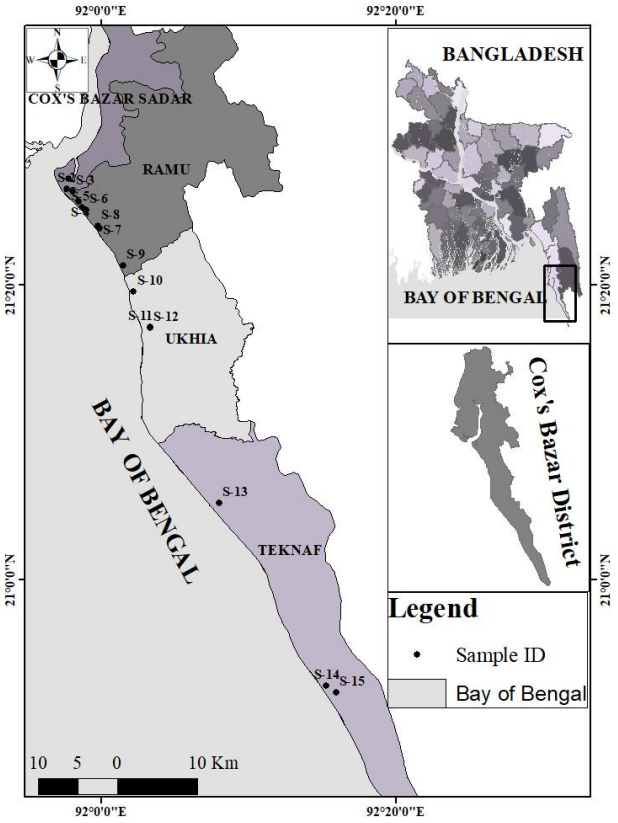

Figure 1. Location map of the study area.

The purpose of this work is to evaluate the principal ion chemistry, hydrochemical facies, and hydrogeochemical processes by applying the Piper plot, Durov plot, Gibbs plot, various bivariate and scatter plots and multivariate statistical approaches.

2.2. Hydrochemical analysis

Fifteen representative groundwater samples were collected from the study region. The procedure for collecting samples was explained in [17]. Onsite measurements of physical parameters were conducted by portable meters (HANNA-HI 9813-5 for pH and temperature and HANNA-HI 8733 for EC and TDS). Portable land Global Positioning System (GARMIN-MAP-64) was used to identify the geographic locations of the chosen wells (Fig. 1). The physico-chemical characteristics of groundwater samples including major cations and anions like calcium (Ca^{2+}), magnesium (Mg^{2+}), sodium (Na^{+}), potassium (K^{+}), bicarbonate (HCO_3^{-}), carbonate (CO_3^{-}), chloride (Cl^{-}), nitrate (NO_3^{-}), and sulfate (SO_4^{2-}), were examined in accordance with the method suggested by the American Public Health Association [27]. An Atomic absorption spectrophotometer (Shimadzu AA 6800) was used to analyze the major cations (Ca^{2+}, Mg^{2+}, Na^{+}, K^{+}), whereas major anions (NO_3^{-}, SO_4^{2-}, and Cl^{-}) were determined by UV-VIS spectrophotometer (Shimadzu UV-3401). Bicarbonate (HCO_3^{-}) concentration was measured by acid titration procedure [28].

The evolution of aquifer quality and the sources of groundwater recharge are commonly examined using conventional hydrogeochemical methods. Piper trilinear plot [29] and the Durov plot [30] of main the cations and anions were used to analyze the chemical components of groundwater samples. The Gibbs plot was used to identify the factors affecting the water quality, such as precipitation, rock weathering, or evaporation.

The hydrogeochemical mechanisms are analyzed using numerous bivariate and scatter diagrams. These diagrams show the intensity and pattern of correlations between the two variables.

2.3. Multivariate statistical analysis

Multivariate statistical approaches such as correlation analysis, principal component analysis (PCA) and hierarchical cluster analysis (CA) were analyzed with SPSS (version 23.0) software, for identify the source of the solutes in the groundwater. Pearson's correlation coefficient was applied to assess the relationship among

physicochemical parameters obtained in groundwater samples. PCA and Hierarchical CA were applied to categories the groundwater depending on their geochemical properties. Principal Component Analysis (PCA) with varimax Kaiser Normalization were chosen for the extraction and rotation methods accordingly. In cluster analysis, Ward's method with squared Euclidean distances is used to produce dendrogram in the investigation, as described by [31].

2.4. Spatial analysis

In this study, spatial analysis was conducted using the Inverse Distance Weighted (IDW) method in ArcGIS (version 10.3).The IDW technique applies a linear accumulation of data scaled with an inverse function of the distance between the place of interest and the measured points to predict the values of an attribute at un-sampled sites [32].

3. Result and Discussion

3.1. Hydrochemistry of groundwater

The measured physicochemical properties of studied groundwater samples are statistically summarized and compared with their corresponding acceptable standards in Table 1. The temperature and pH value ranges from 24°C to 30.3°C (average, 27.93°C) and 7.16 to 8.24 (average, 7.69) correspondingly (Table 1). The temperature reflects the mean temperature of the atmospheric air during the period of the groundwater sampling. The analyzed groundwater has a neutral to mildly alkaline tendency, according to the pH values.

Table 1. Statistical summary of the measured parameters of collected groundwater samples and their comparison with drinking water standards.

Variable	Minimum value n=15	Maximum value	Average value	WHO, 2017	BD Standard (DoE, 1997)
Na^+ (mgL^{-1})	4.57	133.23	41.77	200	200
K^+ (mgL^{-1})	1.09	34.74	6.53	10	12
Ca^{2+} (mgL^{-1})	5.64	219.43	54.37	75	75
Mg^{2+} (mgL^{-1})	3.88	59.47	22.22	50	35
Cl^- (mgL^{-1})	0.68	36.86	5.01	250	600
HCO_3^-(mgL^{-1})	40	276	187.33	300	600
CO_3^{--} (mgL^{-1})	0	48	22.27	-	-
NO_3^-(mgL^{-1})	0.33	36.45	9.61	45	10
SO_4^{2-}(mgL^{-1})	1.66	23.54	7.76	400	400
Temp °C	24	30.3	27.95	-	-
pH	7.16	8.24	7.69	8.5	6.5-8.5
EC (μScm^{-1})	220	3,000	804	1,500	2,000
TDS (mgL^{-1})	143	1950	522.61	500	1000
TH (mgL^{-1})	39.76	734.33	227.21	-	-
HCO_3^-/Cl^-	2.65	109.36	49.92	-	-
SO_4^-/Cl^-	0.44	7.6	2.22	-	-
Na^+/Cl^-	2.2	49.7	21.89	-	-

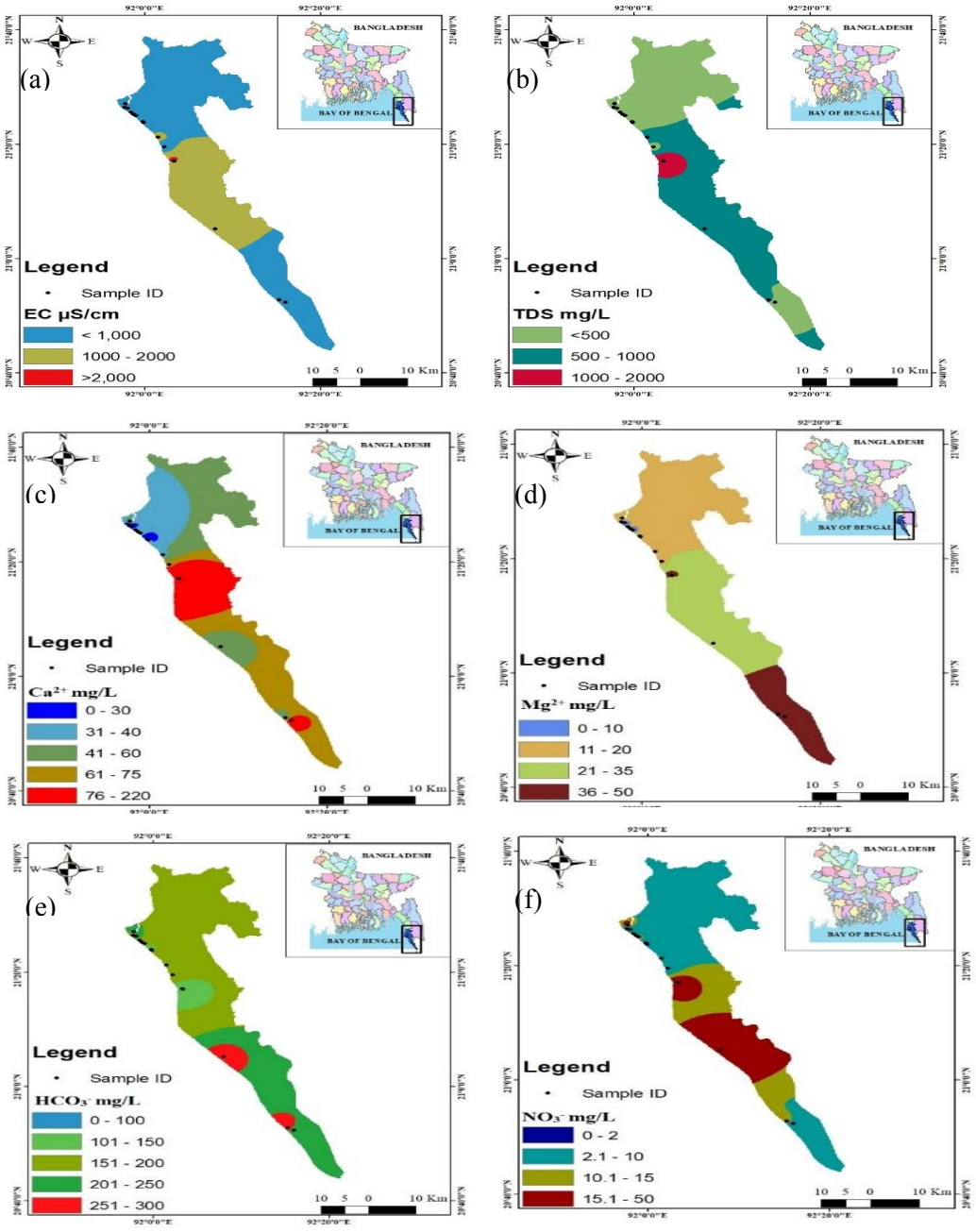

Figure 2. Spatial distribution map of (a) EC, (b) TDS, (c) Ca^{2+} (d) Mg^{2+} (e) HCO_3^- and (f) NO_3^- in the study area

The calculated pH average value of 7.69 is indicative of free CO_2 availability in the examined groundwater, as well as the soluble ions being fully in the form of HCO_3^- ,as temperature and pH are highly influential while the minerals dissolved in groundwater [33]. EC and TDS vary from 270 to 3000 µscm^{-1} (average, 804 µscm^{-1}) and 143 to 1950 mgL^{-1} (average, 522.60 mgL^{-1}) respectively. WHO, 2017 desirable EC and TDS limit (EC, 3000 µscm^{-1}and TDS, 500 mgL^{-1}) is exceeded by 40% of the samples, which belong within the center of the study area, according to the spatial distribution map (Fig. 2a, b). Usually water samples are categorized as brackish water groups with TDS values (TDS > 1000 mgL^{-1}) [33].. Geochemical processes as well as human activities, have influence on EC value [34 - 35].

The cationic dominance pattern is $Ca^{2+} > Na^{+} > Mg^{2+} > K^{+}$ with relative abundances of 43.53%, 33.44%, 17.79%, and 5.22%, respectively. Calcium (Ca^{2+}) is the dominant cation and varies from 5.64 to 219.43 mgL^{-1}, with a mean of 54.37 mgL^{-1}. Only two samples exceed the acceptable limit (75 mgL^{-1}) prescribed by WHO, 2017, and DoE, 1997 [36, 37]. The majority of the sampling sites has greater Ca^{2+} concentrations than Mg^{2+} concentrations, showing the predominance of calcium-bearing materials such as limestone, dolomite, calcite, feldspar, etc. [38] in the sedimentary basins. Ca^{2+} comes from Ca-bearing silicate minerals like K-feldspars, pyroxenes, and amphiboles. The central and southern parts of the study area have higher Ca^{2+} concentrations than the rest, as shown by the spatial distribution in Fig. 2c. Sodium Na^{+} concentration varies from 4.57 to 133.23 mgL^{-1}, with an average value of 41.77 mgL^{-1}, and the entire samples are within WHO and DoE certified limits. Na^{+} could be ascribed to the weathering of rocks, such as sodium plagioclase and halite, as well as the impact of human and animal feces [39]. The Mg^{2+} concentration varies from 3.88 to 59.47 mgL^{-1}, where the average concentration was 41.77 mgL^{-1}. Only one sample exceeds the WHO standard limits (50 mgL^{-1}) for drinking water. In the spatial distribution map (Fig. 2d), Mg^{2+} content shows an increasing trend from north to south throughout the research area. The elevated concentration of Mg^{2+} may be derived from mineral dissolution containing Mg^{2+} as well as industrial and domestic waste that may contribute Mg^{2+} to the groundwater [32]. Potassium (K^{+}) contents vary from 1.09 to 34.74 mgL^{-1}, with a mean value of 6.52 mgL^{-1}. In groundwater, the maximum permissible value of K^{+} is 10.0 mgL^{-1}. Except S-9 and S-12, all the samples fall within the permissible limit set by WHO and BD standard.

The principle anions in groundwater are in the following order $HCO_3^{-} > CO_3^{-} > NO_3^{-} > SO_4^{2-} > Cl^{-}$, with their corresponding contributions of 80.75%, 9.59%, 4.14%, 3.34%, and 2.16%. Bicarbonate (HCO_3^{-}) concentrations vary from 40 to 276 mgL^{-1} (average, 187.33 mgL^{-1}), and are the most predominant anion in the groundwater, followed by CO_3^{-} (0 to 48 mgL^{-1}, average, 22.26 mgL^{-1}), SO_4^{2-}(1.66 to 23.54 mgL^{-1}, average, 7.76 mgL^{-1}), NO_3^{-} (0.33 to 36.45 mgL^{-1}, average, 9.61 mgL^{-1}), and Cl^{-} (0.68 to 36.86 mgL^{-1}, average, 5.01 mgL^{-1}). All the measured parameters in the samples are found below the WHO permitted ranges (Table 1). HCO_3^{-} in subsurface water typically denotes fresh water [40]. The predominance of Ca^{2+} and HCO_3^{-} in groundwater suggests that they come from a similar origin of minerals, such as the dissolution of carbonate minerals like calcite, dolomite, chalk, and limestone [39]. Spatial distribution map (Fig. 2e) shows higher HCO_3^{-} concentration at the central and southern parts. However, about 27% of the sample exceeded the NO_3^{-} concentration limit at the middle part of the study area (Fig. 2f) according to [36] requirement, but it is still below the WHO standard's limit. NO_3^{-} is originated from farming and commercial fields through leaching of plant nutrients, nitrate fertilizers, and home and industrial waste [7].

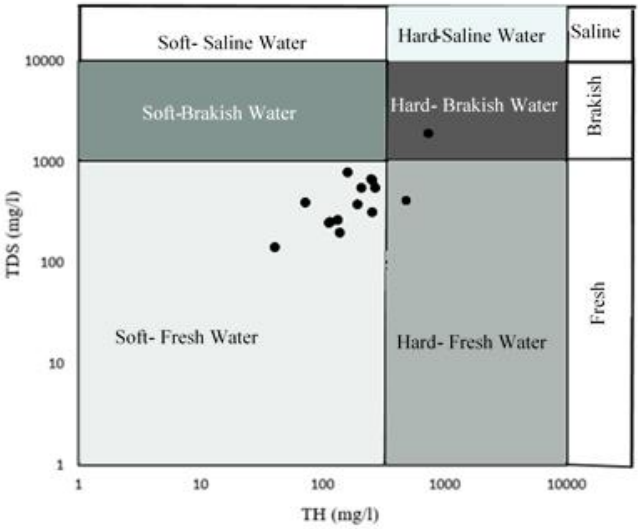

Figure. 3. Groundwater quality in the study area based on TDS and TH [11].

The relatively low SO_4^{2-}concentrations in groundwater samples show that the aquifer is devoid of sulfate-rich minerals like gypsum. The lower sulfate concentration also indicates that the location was not industrial, when higher levels may have been expected due to industrial operations and impurities. In general, Cl^{-} is used as a measure of the quality index of water, and excessive concentrations result in the water being salty and having laxative effects. However, the studied Cl^{-} concentrations are within the WHO drinking water quality

limit, and there is no possibility of salt water intrusion in the aquifer.

Ionic ratios of HCO_3^-/Cl^-(<1.00), SO_4^{2-}/Cl^-(<0.5) and Na^+/Cl^-(<0.86) indicates seawater intrusion in the groundwater [41, 42]. The average HCO_3^-/Cl^-, SO_4^{2-}/Cl^-, and Na^+/Cl^- values are 49.92, 2.22, and 21.88 (Table.1), implying that there is no marine influence in the groundwater within the studied area.

3.2. Hydrochemical facies

The groundwater appropriateness for drinking and household purposes is significantly influenced by its hardness. Total hardness (TH) of water results from the existence of alkaline earths. The following formula after [43] is used to estimate the TH = (2.497 Ca^{2+} + 4.115 Mg^{2+}) in mgL^{-1}. The TH value of the examined sample ranges from 39.76 to 734.32 mgL^{-1}, with a mean value of 227.20 mgL^{-1} and therefore it can be categorized as soft to very hard water [44]. A systematic assessment of groundwater quality based on TDS and TH [11] are represented in Fig. 3, where 87% of the samples are categorized as soft fresh groundwater and 13% is scattered to hard fresh, and hard brackish water. Hydrochemical facies are specific sections that are used to classify the water based on the cation and anion concentration [7, 45].

The cationic and anionic data ($meqL^{-1}$), is expressed with the piper trilinear diagram [29] (Fig. 4). It is a unique arrangement, which is used to determine the groundwater evolution and its chemical association throughout the study area [46]. This plot categorized the groundwater into four different classes, i) Ca^{2+}- Mg^{2+}- Cl^-- SO_4^{2-} , ii) Na^+- K^+- Cl^-- SO_4^{2-} iii) Na^+- K^+- HCO_3^-, iv) Ca^{2+}- Mg^{2+}- HCO_3^- [29, 47]. In the present study, 80% of the samples fall in the Ca^{2+}- Mg^{2+}- HCO_3^- facies field showing that Ca^{2+} and Mg^{2+} alkaline earth metals are major cations and weak acids HCO_3^- is the major anion. 20% of the sample is plotted in Na^+-K^+-HCO_3^- facies, whose chemical associations are controlled by alkalies (Na^+- K^+) and weak acids (HCO_3^-).

Another model was proposed by [30], which features additional information about hydrochemical facies to categorize the water kinds. It showed several potential geochemical processes for analyzing and evaluating the quality of groundwater [48].

Figure 4. Piper diagram representing hydrochemical facies based on major ion composition of groundwater

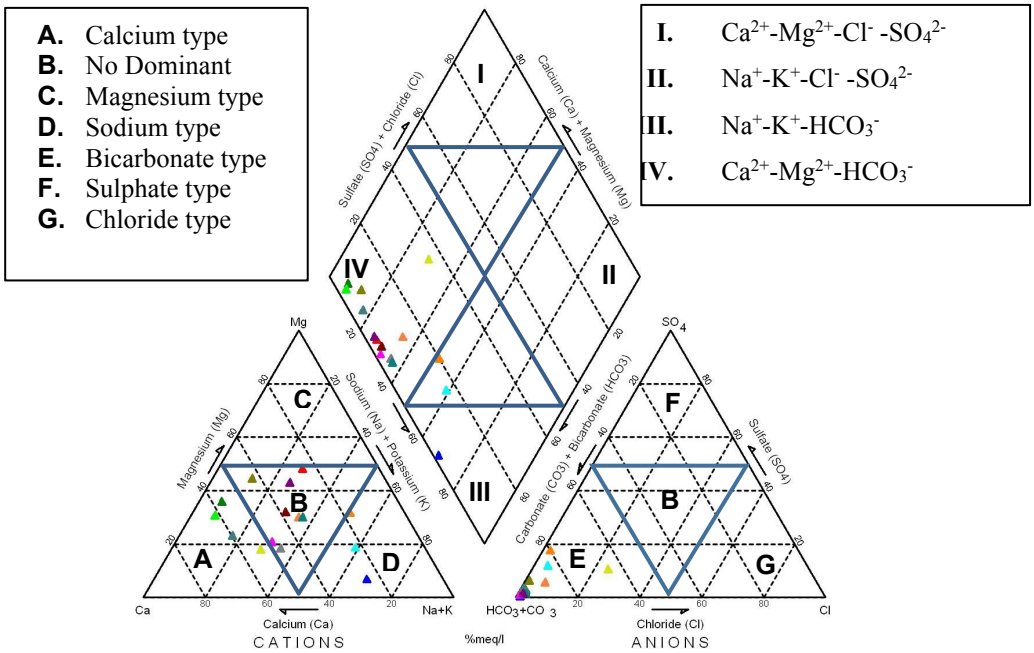

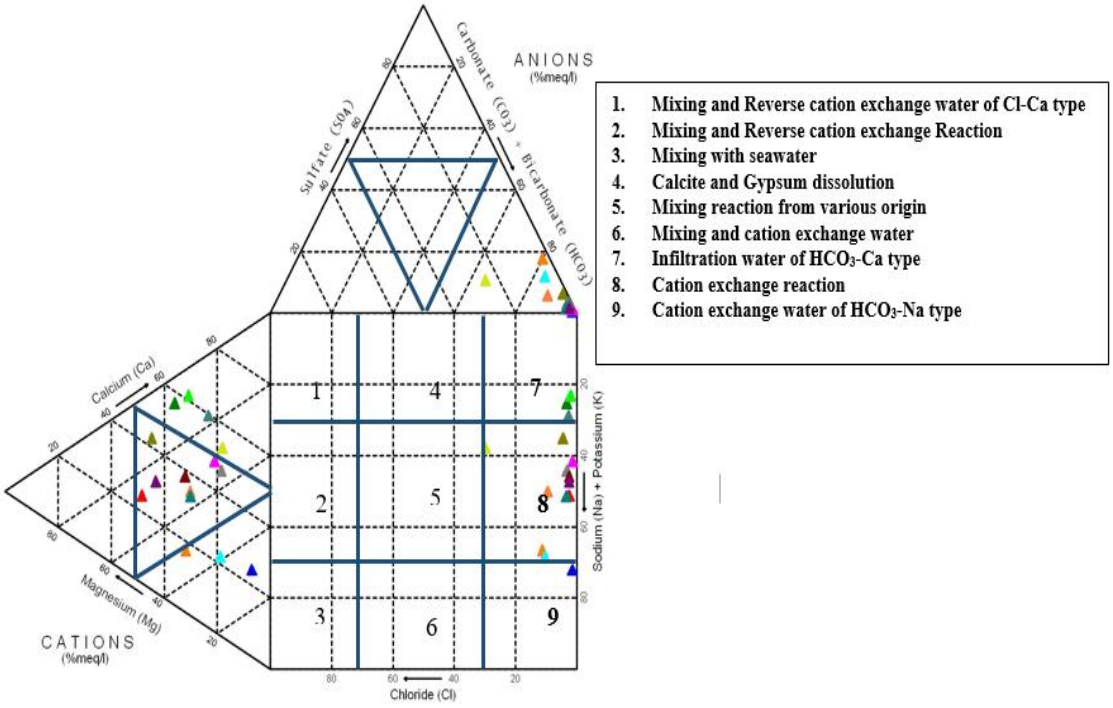

Figure 5. Durov diagram showing hydrochemical processes of groundwater along the studied area.

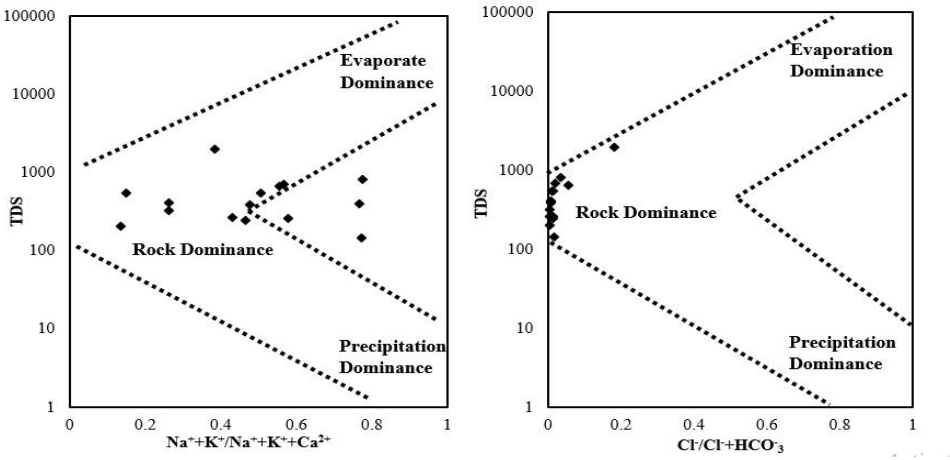

Figure 6. Gibbs plot [50] (a) TDS versus Na^++ K^+/ Na^++K^++Ca^{2+} and (b) TDS versus Cl^-/Cl^-+HCO_3^- indicating the mechanisms controlling the groundwater chemistry

The Durov diagram displays the major cation and anion plot. In the present Durov diagram (Fig. 5), water samples are concentrated in the HCO_3^- domain of the anionic triangle, representing the carbonate weathering zone. On the other hand, in the cationic triangle, samples are scattering within the Ca^{2+}, intermediate and Na^+ + K^+ water type domain. This ion distribution is consistent with the Ca^{2+}- Mg^{2+}- HCO_3^- and Na^+- K^+ - HCO_3^- facies of the Piper plot. In the Durov diagram, 73% of the samples are traced in the cationic exchange fields of 8, where Ca^{2+}- HCO_3^- is prevalent combined with dolomite and an important ion exchange is assumed when Na^+ is dominant. 13% of samples are distributed in field 7, which is in accordance with the features of modern infiltration of Ca^{2+}- HCO_3^- type water and the remaining one in field 9 of Na^+- HCO_3^- type water [49].

3.3. Hydrogeochemical evaluation

3.3.1. Gibbs plot

Gibbs plot [50] explains the process and mechanism that control the groundwater chemistry (Fig. 6). The observed groundwater samples are placed within the rock dominance domain, revealing rock–water interaction is the major natural process that influences water chemistry. Furthermore, precipitation and evaporation have no impact on groundwater. Weathering of rock, dissolution of carbonate, precipitation, and ion exchange among water and clay-rich minerals characterize the rock-water interaction zone [51].

Na-normalized Ca vs Na-normalized Mg^{2+} and HCO_3^- (Fig. 7a, b) is prepared according to [52] to evaluate the corresponding influence of the three main weathering mechanisms (silicate, carbonate, and evaporite) that control the concentration of solute in groundwater. According to these plots, the majority of the samples is intermediate between global average silicates and carbonate weathering.

3.3.2. Rock water interaction

Carbonate weathering

Carbonate weathering is a significant geochemical mechanism in groundwater when Ca^{2+} and Mg^{2+} are the main ions with their mean contributions of 70% to the total cations. On the other hand, $HCO_3^- + CO_3^-$ is the dominant anion with an average contribution of 92% to the total anions. Ionic concentrations that are plotted above the 1:1 line in the (Ca^{2+}+ Mg^{2+}) versus ($SO_4^{2-} + HCO_3^-$) scatter diagram are produced from carbonate weathering, while those on the 1:1 equiline are affected by the two carbonate and silicate weathering [53]. 67% of the projected points fall along the 1:1 equiline in (Ca^{2+} Mg^{2+}) versus (SO_4^{2-}+HCO_3^-) scatter diagram (fig. 8a), reflecting both the carbonate (calcite/dolomite) and silicate weathering [53]. Additionally, 26% of samples are below the 1:1 trend on the (Ca^{2+}+ Mg^{2+}) vs. ($HCO_3^- + SO_4^{2-}$) diagram, indicating carbonate weathering in the groundwater system [54]. Only one sample S-3, shifted to the (HCO_3^-+ SO_4^{2-}) domain, indicating the involvement of a normal ion exchange mechanism [54].

The (Na^+) versus (HCO_3^-) bivariate plot is utilized to determine the prevalence of silicate/carbonate weathering in groundwater. The concentration of HCO_3^- in groundwater rises as a result of carbonate weathering. It is strongly assisted by groundwater with a high concentration of HCO_3^- exceeding Na^+ concentration [8].

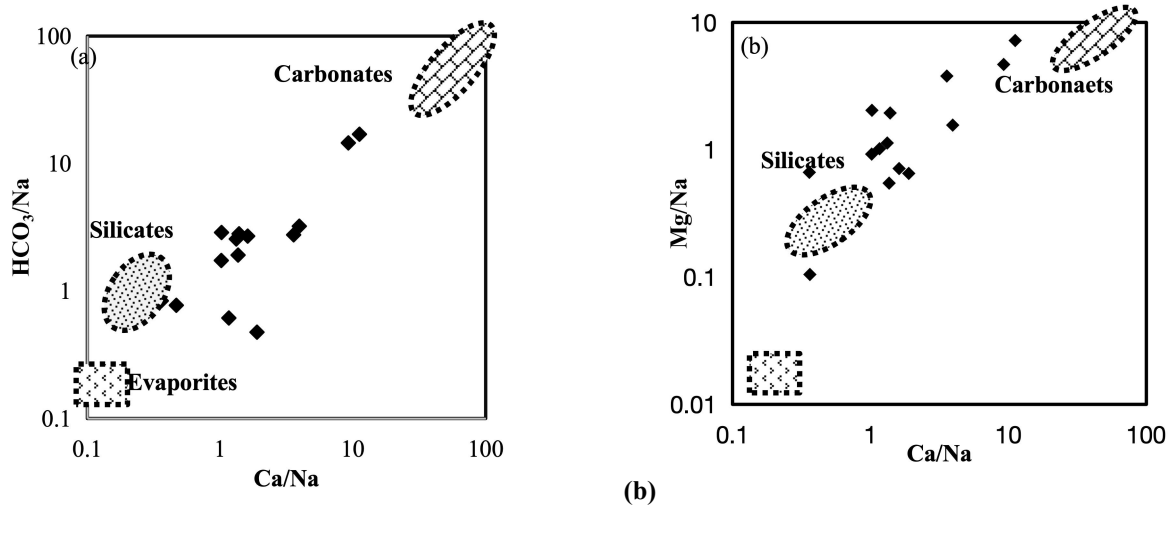

(a) **(b)**

Figure 7. Bivariate plots of a) Na^+ normalized HCO_3^- and Ca^{2+}, b) Na^+-normalized Mg^{2+} and Ca^{2+}, presenting the trends of weathering. The dotted areas show global average compositions of groundwater in term of evaporite dissolution, silicate weathering, and carbonate dissolution without mixing following [52].

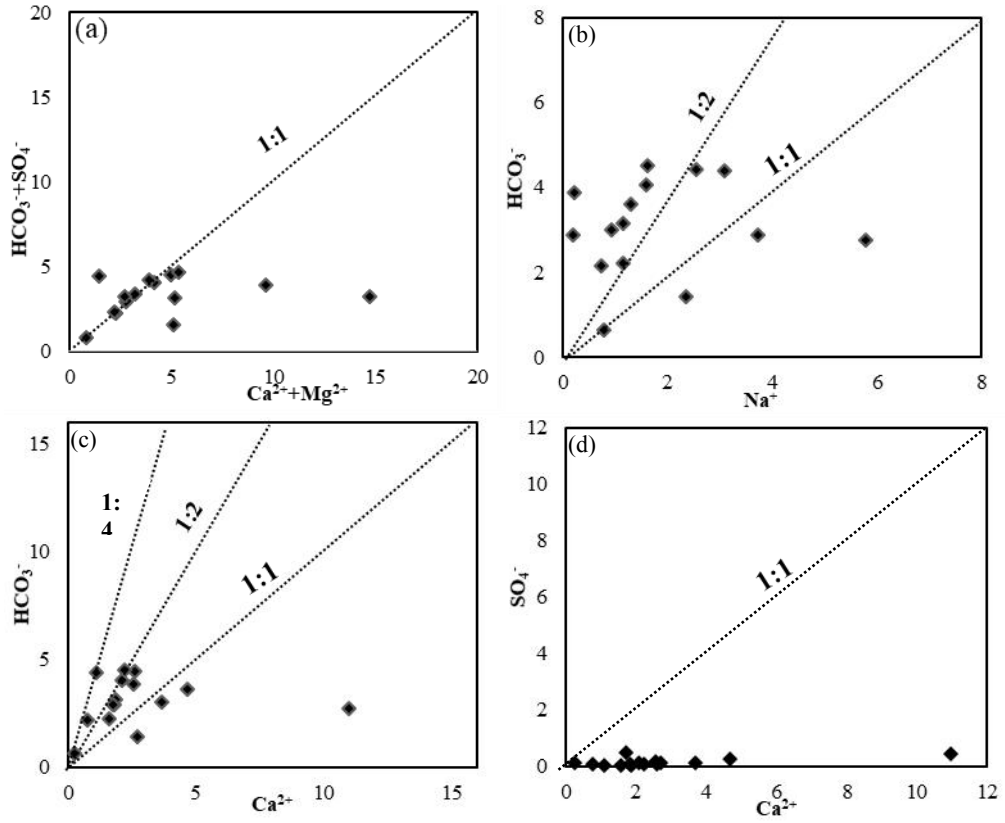

Figure 8. Bivariate plots of (a) $Ca^{2+}+Mg^{2+}$ versus $HCO_3^-+SO_4^-$, (b) Na^+ versus HCO_3^-, (c) Ca^{2+} versus HCO_3^- and (d) Ca^{2+} versus SO_4^-.

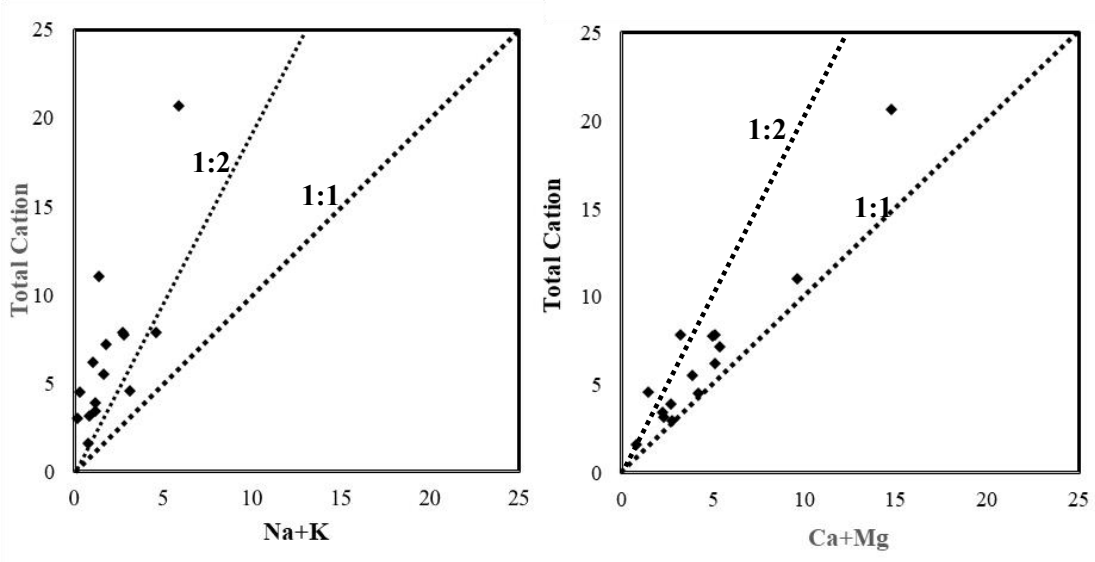

Figure 9. Bivariate plots of (a) $Na^+ + K^+$ versus Total Cations and (b) $Ca^{2+} + Mg^{2+}$ versus Total Cations indicating Carbonate/Silicate weather.

The elevated Na^+ level in the groundwater above alkalinity demonstrates the action of ion exchange. The Na^+ versus HCO_3^- plot shows that almost 80% of the samples fall above the equiline, indicating carbonate weathering is a dominant process in groundwater (Fig. 8b). Few samples are below the equiline showing a higher Na^+ content than HCO_3^-, indicating the effect of ion exchange in the aquifers.

In groundwater, the impact of cation exchange, chemical weathering, as well as evaporation, can be explained by the HCO_3^- vs. Ca^{2+} plot. The corresponding Ca^{2+} and HCO_3^- ratio will be 1:2 when calcium and bicarbonate are derived primarily from calcite, but it will be 1:4 in the case of dolomite weathering [54]. The Ca^{2+} versus HCO_3^- scatter plot reveals that the majority of the samples are below the 1:2 line, suggesting calcite weathering (Fig. 8c). Few samples lie close to the 1:4 line, assuming dolomite weathering. Ca^{2+}: SO_4^{2-} ratio is around 1:1 when sulfuric acid acts as a weathering agent [55]. On the scatter plot of Ca^{2+} versus SO_4^{2-} (Fig. 8d), all of the samples went below the 1:1 trend line, which strongly demonstrates the superiority of calcite weathering over dolomite weathering in the presence of sulfuric acid.

Silicate weathering

Silicate weathering is a fundamental geochemical mechanism that governs the main ion chemistry of groundwater [56]. The Na^+ content in groundwater in the area is accountable for silicate rocks weathering. The role of cation to the proportion of $(Na^+ + K^+)$/Total cations could be applied to determine groundwater that go through silicate weathering [57, 58]. The samples lie above the 1:2 equiline, showing little silicate (alkali feldspar) weathering, while samples tend along the $Na^+ + K^+$ = 1:1 line, representing silicate weathering, that provides primarily Na^+ and K^+ to groundwater [57]. $Na^+ + K^+$ versus total cation diagram indicates that maximum groundwater samples are above the 1:2 equiline, showing the lack of silicate weathering (Fig. 9a). Only a few samples go towards the $Na^+ + K^+$ = 1:1 line, revealing that silicate weathering has a lesser contribution.

The silicate weathering is also determined by $Ca^{2+}+Mg^{2+}$ versus total cations plot. In the $Ca^{2+}+Mg^{2+}$ versus total cations plot, the majority of the samples exhibit a linear distribution along the 1:1 equiline, indicating that calcium and magnesium-rich minerals have weathered as well as less influence of silicate weathering (Fig. 9b). Some samples exceed the 1:2 equiline, indicating the enrichment of alkali feldspar [54].

Ion exchange

Ion exchange is a significant hydrochemical phenomenon of the aquifer where ions interchange their places based on the aquifer's conditions. Chloro-alkaline Indices CAI-I and CAI-II have been determined with equation 1 and 2, and the results are presented in Fig. 10.

$$CAI\text{-}1 = Cl^- - (Na^+ + K^+)/Cl^- \quad \text{.....(1)}$$

$$CAI\text{-}II = Cl^- - (Na^+ + K^+)/SO_4^{2-} + HCO_3^- + CO_3^- + NO_3^- \quad \text{.....(2)}$$

Major ion concentrations are shown in $meqL^{-1}$. Positive value implies an exchange between Na^+ or K^+ with Mg^{2+} or Ca^{2+} in the groundwater, and negative indices value implies a cation-anion exchange process in chloro-alkaline disequilibrium condition [59]. All the groundwater samples are showing dominant cation-anion exchange with negative value.

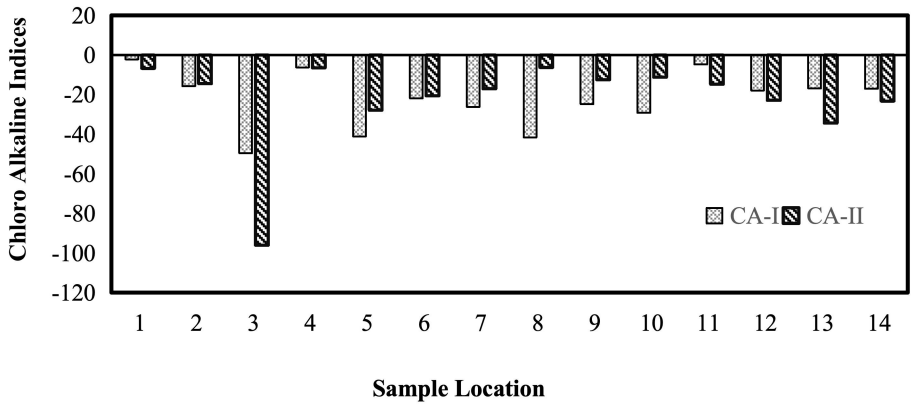

Figure 10. Bar diagram of Chloro-Alkaline Indices CAI-I and CAI-II for the groundwater samples from the study area.

Table. 2. Pearson correlation matrix of the hydrochemical parameters of groundwater (significant values (>0.5) are in bold type face).

Variable	Na^+	K^+	Ca^{2+}	Mg^{2+}	Cl^-	HCO_3^-	CO_3^{2-}	NO_3^-	SO_4^{2-}	pH	EC	TDS
Na^+	1.00											
K^+	0.44	1.00										
Ca^{2+}	.658**	-0.02	1.00									
Mg^{2+}	0.34	0.12	.669**	1.00								
Cl^-	.814**	0.11	.899**	0.46	1.00							
HCO_3^-	0.10	-0.03	0.09	0.25	-0.03	1.00						
CO_3^{2-}	-0.27	0.00	-0.36	-0.06	-0.32	.631*	1.00					
NO_3^-	0.01	0.30	-0.07	0.10	-0.04	-0.01	0.27	1.00				
SO_4^{2-}	.664**	.613*	.618*	0.49	.655**	-0.09	-0.40	-0.13	1.00			
pH	-0.32	-.515*	-0.43	-.664**	-0.28	-0.12	0.16	-0.31	-.610*	1.00		
EC	.871**	0.31	.873**	.535*	.964**	0.09	-0.20	0.11	.721**	-0.42	1.00	
TDS	.871**	0.31	.873**	.535*	.964**	0.09	-0.20	0.11	.721**	-0.42	1.000**	1.00

** Correlation is significant at the 0.01 level (2-tailed).

* Correlation is significant at the 0.05 level (2-tailed).

Note: EC-Electrical Conductivity; TDS-Total Dissolved Solid

Table3. Varimax rotated principal component analysis (R-mode) of water quality parameters (significant values (>0.5) are in bold type face)

Parameters	PCA 1	PCA 2	PCA 3
Na^+	**0.839**	-0.109	0.262
K^+	0.216	-0.148	**0.892**
Ca^{2+}	**0.939**	-0.032	-0.222
Mg^{2+}	**0.66**	0.258	-0.023
Cl^-	**0.947**	-0.134	-0.053
HCO_3^-	0.155	**0.876**	-0.049
NO_3^-	-0.038	0.262	**0.648**
SO_4^{2-}	**0.747**	-0.331	0.321
CO_3^{2-}	-0.27	**0.86**	0.201
EC	**0.969**	-0.012	0.157
TDS	**0.969**	-0.012	0.157
Eigenvalue	5.644	1.779	1.41
% of Variance	51.312	16.172	12.82
Cumulative %	51.312	67.484	80.304

Note: PCA-Principal Component Analysis

3.4. Multivariate Statistical analysis

3.4.1. Correlation Coefficient

TDS is strongly correlated to sodium (Na^+), calcium (Ca^{2+}), magnesium (Mg^{2+}), chloride (Cl^-), and sulfate (SO_4^{2-}) concentrations with correlation coefficients of 0.871, 0.873, 0.535, 0.964, and 0.721 correspondingly, representing their contribution to water mineralization (Table 2). The strong positive connection among Na^+, Ca^{2+}, Cl^-, and SO_4^{2-} implies that they are derived from the common origin. Cl^- and Na^+ show a significant connection(r=0.941), indicating their similar

source. Mg^{2+} is positively associated with Ca^{2+} (r=0.855), the existence of Mg^{2+} in this groundwater may be attributed to rock weathering. It implies that a rise in the concentration of one parameter might have an effect on the concentration of another parameter and seems to have a common origin. SO_4^{2-} contents are closely related to Ca^{2+}, Na^+ and K^+, which is described by evaporate mineral dissolution and cation exchange in clay minerals. Nitrates show no association with the major anion and cation or TDS, revealing that they are derived from anthropogenic sources.

3.4.2. Principal Component Analysis PCA

PCA was used to assess water quality metrics including EC, TDS, Na^+, K^+, Ca^{2+}, Mg^{2+}, Cl^-, SO_4^{2-}, NO_3^-, HCO_3^- and CO_3^- with the aim of distinguish different processes affectingthe hydrogeochemistry. In order to better understand the potential influences on the water systems, the sum of the variance of the component coefficients was maximized using varimax rotation [60, 61].These variables are organized into three primary PCAs that collectively explain 87% of the variables of the data set (Table 3). The scree plot is utilized to decide how many PCAs should be taken to explain the frameworks of the estimated cases and only variables with eigenvalues greater than one are chosen (Fig. 11a). The first three PCAs addressed more than 80.30% of the variance within the groundwater variables (Fig. 11b).

PCA 1, has a eigenvalue of 5.64, representing 51.31% of the entire variable and strongly positively loaded (>0.75) with TDS, EC, Na^+, Ca^{2+}, Cl^-, Mg^{2+} and SO_4^{2-}. The significant loading of Na^+ (.839) could be attributed to feldspar weathering or cation exchange [62]. Calcium (Ca^{2+}) has a heavy loading of 0.939, which could be related to the weathering/dissolution of silicate minerals (e.g., amphiboles, feldspars, and pyroxenes), whereas high loadings of Na^+ and Cl^- (0.839 and 0.947) are most probably related to natural (mild) salinity, a procedure supported by the high positive correlation. There are various environmental sources of sodium and chloride content, including atmospheric deposition, rock-water interaction, and saltwater incursion [63]. Mg^{2+} (0.66) loading suggest the primary weatheringprocesses e.g., alluminosilicates weathering, on groundwater chemistry. The dissolution of gypsum mineral may raise the SO_4^{2-} (0.747) content in groundwater [64]. Furthermore, intensive groundwater extraction leads to SO_4^{2-} leakage into groundwater. SO_4^{2-} in groundwater can also be associated with atmosphere deposition [65]. The enhanced dissolved minerals in water resulted in the high EC and TDS values [66]. TDS and EC have a significant positive association with the principal cations and anions, and the high loadings of TDS, EC with Na^+, Ca^{2+}, Cl^-, and SO_4^{2-} (Table 3) represent their considerable influence on the total mineralization in the examined groundwater. As a result, PCA 1 might be viewed as rock water interaction and natural salinity following silicate weathering.

PCA 2 shows a lower eigenvalue (1.77) and (16.17%) variance and is distinguished by significant factor loadings of HCO_3^- (.876) and CO_3^- (.861). The HCO_3^- and CO_3^- might be explained by carbonate (aragonite, calcite, and dolomite) dissolution, or they could be produced by bacterial breakdown of organic contaminants [39, 67] as well as by surface water leaking to aquifers.

PCA 3 exhibits an eigenvalue of 1.41 which comprises 12.82% of the overall variance, is heavily loaded with K^+ (0.892) and NO_3^- (0.648), which are weathering byproducts of silicate minerals, clay minerals such as illite may adsorb K^+ ions during silicate weathering [68]. This could explain the reduced factor loading of K^+ in PC1. Anthropogenic sources, such as intensive farming incorporating the extensive use of pesticides and fertilizers, raise the NO_3^- levels in shallow groundwater via infiltration [69]. The correlations among the investigated variables are also observed in the PCA 1 versus PCA 2 and PCA 1 versus PCA 3 plots. Whereas the component plot (Fig. 12a) demonstrates that TDS and EC have a significant correlation. The correlation among EC, TDS, Cl^-, Na^+, Ca^{2+}, Mg^{2+} and SO_4^{2-} is displayed in the PCA 1 versus. PCA 2 diagram (Fig. 12a). Corresponding clustering is also noticed in PCA 1 vs. PCA 3 (Fig. 12b) plot, in which PCA 3 is loaded with K^+ and NO_3^-.

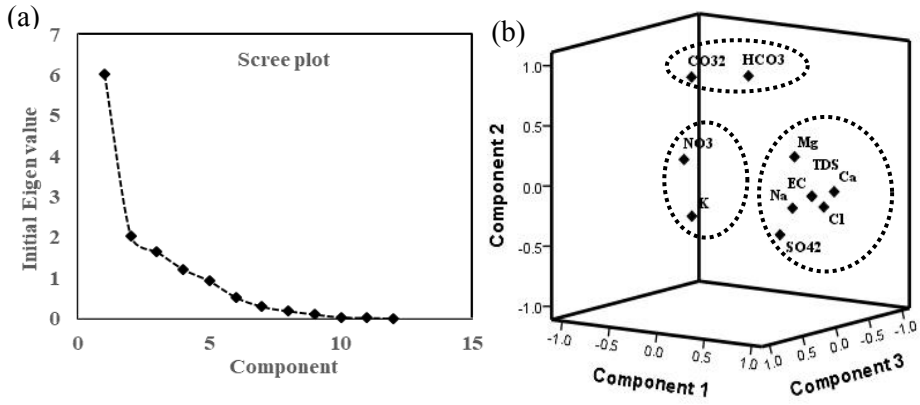

Figure 11. Principal component analysis by (a) scree plot (eigenvalues) and (b) component plot in rotated space

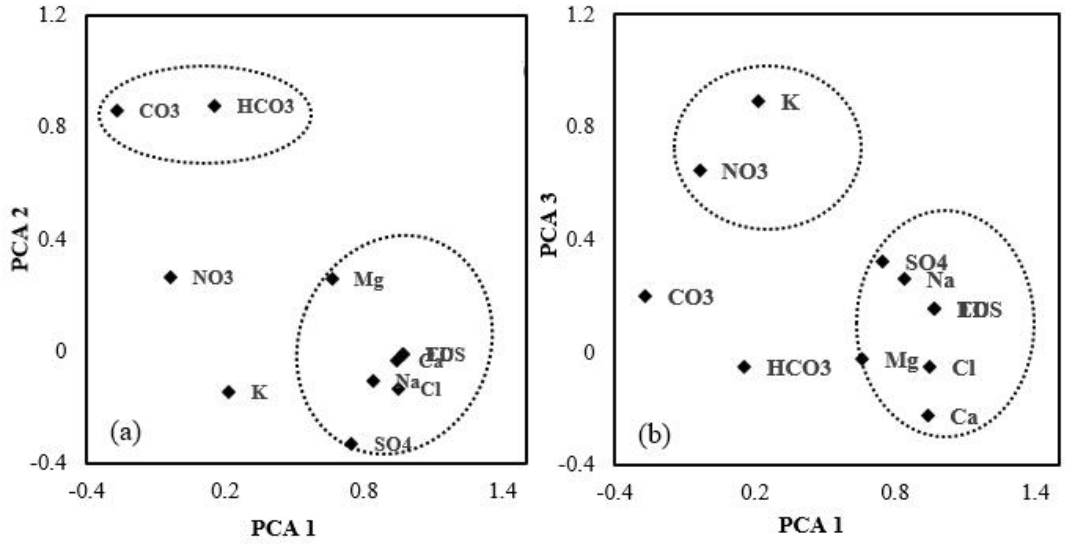

Figure 12. Plots of first three principal component loadings (a) PCA 1 versus PCA 2 and (b) PCA 1 versus PCA 3 for analyzed groundwater parameter.

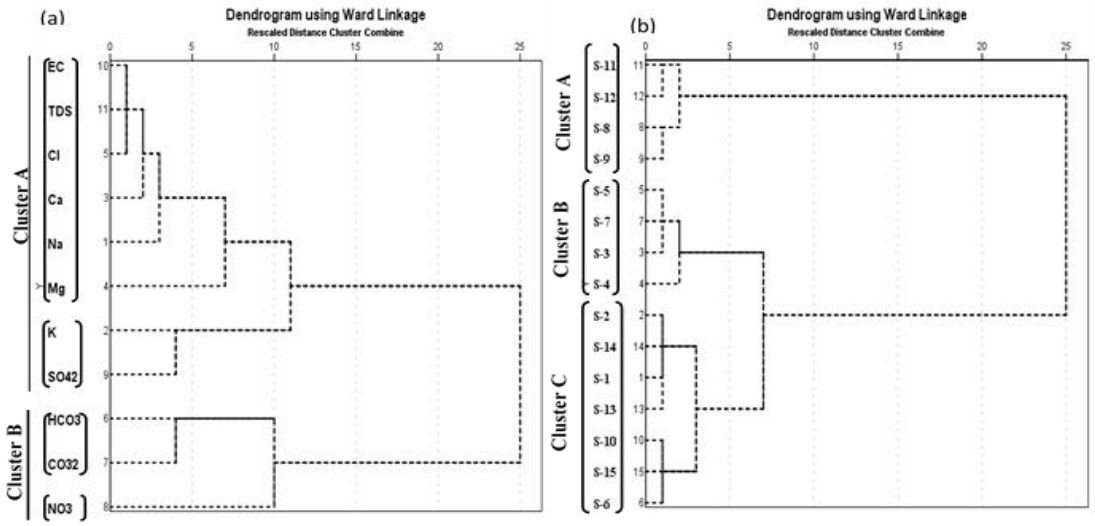

Figure 13. Dendrogram showing the hierarchical clusters of a) analyzed hydrochemical parameters and (b) sampling sites.

3.4.3. Cluster Analysis CA

Hierarchical cluster analysis (CA) has been carried out, and the outcomes are quite similar to those of the PCA. The hierarchical cluster analysis (HCA) produces a dendrogram of hydrogeochemical data shows two clusters (Fig. 13a). Cluster A is split into two distinct sub-clusters. The sub-cluster 1 was made up of EC, TDS, Cl^-, Ca^{2+} and Na^+ loosely attached with Mg^{2+}. This cluster can be regarded as geogenic processes regulated by rock-water interaction and natural salinity. This corresponds to PCA 1. The second sub-cluster suggests K^+ and SO_4^{2-} similarities, which corresponds to factors 1 and 3 in PCA. These can be regarded as both natural and anthropogenic activities, coming from fertilizers and pesticides used in farming. Cluster B is made up of two distinct sub-clusters. Sub cluster 1 contains HCO_3^- and CO_3^-, signifying carbonate weathering, whereas sub cluster 2 contains NO_3^- from an anthropogenic source. This cluster correlates to PCA 2 and PCA 3.

Table 4. Mean values of chemical parameters for each cluster.

Parameters	Cluster A	Cluster B	Cluster C
Na^+	72.7825	34.7275	28.07857
K^+	13.95	1.7325	5.03
Ca^{2+}	78.6525	34.7	51.74
Mg^{2+}	24.555	11.6325	26.93857
Cl^-	12.26	1.6225	2.81
HCO_3^-	118	221	207.7143
CO_3^-	7.5	23.5	30
NO_3^-	12.095	0.9575	13.14429
SO_4^{2-}	14.615	3.48	6.291429
Temp	28.425	26.65	28.42857
pH	7.5575	7.9675	7.611429
EC	1367.5	482.5	665.7143
TDS	888.875	313.65	432.7143

Q-mode CA was conducted in order to assess the resemblance and clustering within the sample location. Sampling sites that correspond to a given cluster possess certain properties in relation to the investigated parameters [70]. Three significant clusters were identified from all of the examined variables for the 15 sampling sites (Fig. 13b). Cluster A exhibits four (S-11, S-12, S-8, S-9) sampling location, cluster B also includes four (S-5, S-7, S-3, S-4) as well as cluster C has seven (S-2, S-14, S-1, S-13, S-10, S-15, S-6) sampling sites.

Table 4 illustrates the mean concentrations of the investigated water quality metrics in the three classified categories. Cluster A presents a significant concentration of EC, TDS, Na^+, Ca^{2+}, Cl^-, and SO_4^{2-}, indicating rock water interaction and natural saltiness in the aquifer system. The highest HCO_3^- and CO_3^- values in Cluster B, which comprises S-3, S-4, S-5 and S-7, indicate carbonate weathering in the aquifer system. Cluster C has the lowest values for most of the parameters with the exception of HCO_3^-, CO_3^-, Mg^{2+}, and NO_3^- suggesting that carbonate weathering is occurring in conjunction with anthropogenic sources of NO_3^-.

4. Conclusion

This study emphasizes on groundwater hydrogeochemistry and drinking water suitability from the southeast coastal aquifer of Bangladesh. The predominance of cation and anion contents is within the order of $Ca^{2+}>Na^+>Mg^{2+}>K^+$ and $HCO_3^- > CO_3^- > NO_3^- > SO_4^{2-} > Cl^-$ respectively. Maximum physicochemical parameters satisfy the WHO's, 2017 drinking water quality standard, and there are no noticeable water quality differences in the study area due to geochemical variation. These two Ca^{2+}-Mg^{2+}- HCO_3^- and Na^+-K^+-HCO_3^- hydrochemical facies are dominant in this region. The Gibbs plot revealing rock–water interaction is the major natural process regulating groundwater chemistry, where precipitation and evaporation have no substantial impact. Numerous bivariate and scatter plots of weathering and dissolving show that carbonate weathering is the principal process for discharging these ions. Additionally, it indicates that there is ongoing weathering of carbonates containing minerals such as calcite, dolomite, and gypsum within the research area. The PCA analysis implies that weathering and leaching of parent rocks is the principal geogenic source for emitting cations and anions in groundwater

that is well in accordance with the Gibbs plot. Furthermore, anthropogenic activities (such as insecticide and fertilizer use) may have an impact on the hydrogeochemistry of groundwater. Therefore, this research work will serve as a reference data for the area and might be taken into account for future planning of groundwater management for drinking purposes.

Authors Contribution

Material Conceptualization and preparation: NafisaTamannaya Dina, Mohammad Zafrul Kabir, Farah Deeba and Syed Hafizur Rahman; Data collections (on field): Mohammad Zafrul Kabir, Farah Deeba and Nafisa Tamannaya Dina; Formal Analyses: NafisaTamannaya Dina, Farah Deeba, Md. Ferdous Alam and Salma Sultana; Writing-original draft preparation: Nafisa Tamannaya Dina and Farah Deeba. Review and editing: Mohammad Zafrul Kabir, Syed Hafizur Rahman and Md. Golam Rasul. All the authors read and approved the final manuscript.

Conflicts of Interest

There are no conflicts of interest reported by the writers.

Funding

The authors declare that this research did not receive any specific grant from any public or private funding agencies.

Acknowledgment

The authors are thankful to the authority of Bangladesh Atomic Energy Commission for logistic assistance. Sincere appreciation is obligated to the local administration and people for their logistic support and cooperation during the field work.

Data Availability statement

The data presented in this study are available on request from the corresponding author.

REFERENCES

1. Al Naeem, M.F.A., et al., A study on the impact of anthropogenic and geogenic factors on groundwater salinization and seawater intrusion in Gaza coastal aquifer, Palestine: An integrated multi-techniques approach, 2019. 156. p. 75-93.
2. Rahman, M.M., et al., Emerging trends of water quality monitoring and applications of multivariate tools. Water Engineering Modeling and Mathematic Tools, 2021. p. 271-283.
3. Rakib, M., et al., Groundwater salinization and associated co-contamination risk increase severe drinking water vulnerabilities in the southwestern coast of Bangladesh. Chemosphere, 2020. 246. p. 125646.
4. Thilagavathi, R., et al., A study on groundwater geochemistry and water quality in layered aquifers system of Pondicherry region, southeast India. Applied water science, 2012. 2: p. 253-269.
5. Domenico, P.A., Concepts and models in groundwater hydrology. (1972).
6. Aly, A.A., Al-Omran, A.M. and Alharby, M.M., The water quality index and hydrochemical characterization of groundwater resources in Hafar Albatin, Saudi Arabia. Arabian Journal of Geosci, 2015. 8. p. 4177-4190.
7. Ahmed, N., et al., Hydrogeochemical evaluation and statistical analysis of groundwater of Sylhet, north-eastern Bangladesh. Acta Geochim, 2019. 38. p. 440-455.
8. Lakshmanan, E., Kannan, R. and Kumar, M.S., Major ion chemistry and identification of hydrogeochemical processes of ground water in a part of Kancheepuram district, Tamil Nadu, India. Environmental geosciences, 2003. 10(4). p. 157-166.
9. Rajmohan, N. and Elango, L., Identification and evolution of hydrogeochemical processes in the groundwater environment in an area of the Palar and Cheyyar River Basins, Southern India. Environmental Geology, 2004. 46. p. 47-61.
10. Frengstad, B., Banks, D. and Siewers, U., The chemistry of Norwegian groundwaters: IV. The pH-dependence of element concentrations in crystalline bedrock groundwaters. Science of the Total Environment, 2001. 277(1-3). p. 101-117.
11. Kumar, P.S., Evolution of groundwater chemistry in and around Vaniyambadi industrial area:

differentiating the natural and anthropogenic sources of contamination. Geochemistry, 2014. 74(4). p. 641-651.

12. Hossain, A.M., Fien, J. and Horne, R., Megacity Dhaka:'water security syndrome'and implications for the scholarship of sustainability. Sustainable Water Resources Management, 2018. 4. p. 63-78.
13. Giri, S. and Singh, A.K., Human health risk assessment via drinking water pathway due to metal contamination in the groundwater of Subarnarekha River Basin, India. Environmental monitoring and assessment, 2015. 187(3). p. 63.
14. Bodrud-Doza, M., et al., Characterization of groundwater quality using water evaluation indices, multivariate statistics and geostatistics in central Bangladesh. Water science, 2016. 30(1). p. 19-40.
15. Faillat, J. and C.J.H.S.J.H. Drogue, Hydrochemical Differentiation of Superposed Aquifers in Weathered and Decayed Rock and Fractures in Granitic Basement(Differenciation Hydrochimique de Nappes Superposees d'Alterites et de Fissures en Socle Granitique). Hydrological Sciences Journal HSJODN ,1993. 38(3).
16. Hasan, M., et al., Heavy metals distribution and contamination in surface water of the Bay of Bengal coast. Cogent Environmental Science, 2016. 2(1). p. 1140001.
17. Deeba, F., et al., Heavy metals distribution and contamination in groundwater of the south eastern coastal area of Bangladesh. Journal of Water and Environment Technology, 2021. 19(5). p. 267-282.
18. Kabir, M.M., et al., Characterization of groundwater hydrogeochemistry, quality, and associated health hazards to the residents of southwestern Bangladesh. Environmental Science and Pollution Research, 2021. 28(48). p. 68745-68761.
19. Raknuzzaman, M., et al., Assessment of trace metals in surface water and sediment collected from polluted coastal areas of Bangladesh. Journal of water and environment technology, 2016. 14(4). p. 247-259.
20. Islam, A.R.M.T., et al., Drinking appraisal of coastal groundwater in Bangladesh: An approach of multi-hazards towards water security and health safety. Chemosphere 2020. 255. p. 126933.
21. Fatema, S., et al., Seawater intrusion caused by unmanaged groundwater uses in a coastal tourist area, Cox's Bazar, Bangladesh. Environ Earth Sci, 2018. 77. p. 1-13.
22. Seddique, A.A., H. Masuda, and A.J.A.J.o.G. Hoque, Radionuclide and heavy metal contamination in the paleobeach groundwater, Cox's Bazar, Bangladesh: potential impact on environment. Arabian Journal of Geosciences, 2016. 9. p. 1-12.
23. Seddique, A.A., et al., Hydrogeochemical and isotopic signatures for the identification of seawater intrusion in the paleobeach aquifer of Cox's Bazar city and its surrounding area, south-east Bangladesh. Groundwater for Sustainable Development, 2019. 9. p. 100215.
24. Zakaria, M., et al., Developing Conceptual Aquifer Geometry, Structural Geological Control and Possibility of Sea Water Intrusion in Cox's Bazar Area of Bangladesh. IOSR Journal of Applied Geology and Geophysics, 2015. 3(6). p. 21-28.
25. Curray, J.R. and Moore, D.G., Sedimentary and tectonic processes in the Bengal deep-sea fan and geosyncline. In The geology of continental margins, Berlin, Heidelberg: Springer Berlin Heidelberg, 1974. p. 617-627.
26. Alam, M., et al., Geological map of Bangladesh: Dhaka. Geological Survey of Bangladesh. (1990).
27. Ravenscroft, P. and McArthur, A.G., Mechanism of regional enrichment of groundwater by boron: the examples of Bangladesh and Michigan, USA. Applied Geochemistry, 2004. 19(9). p. 1413-1430.
28. APHA (1998) Standard Methods for the Examination of Water and Wastewater. American Public Health

Association, AWWA and WPCF, 20th edn. Washington DC, USA.

29. Das, T.K., et al., Multivariate statistics and hydrogeochemistry of deep groundwater at southwestern part of Bangladesh. Heliyon, 2022. 8(10).
30. Piper, A.M., Transactions American Geophysical Union, A graphic procedure in the geochemical interpretation of water-analyses. Eos, Transactions American Geophysical Union, 1944. 25(6). p. 914-928.
31. Durov, S. Natural waters and graphic representation of their composition. in Dokl Akad Nauk SSSR. (1948).
32. Lattin, J., Green, P. and Carroll, J., Analyzing Multivariate Data Duxbury Press. (2003).
33. Bodrud-Doza, M., et al., Hydrogeochemical investigation of groundwater in Dhaka City of Bangladesh using GIS and multivariate statistical techniques. Groundwater for Sustainable Development, 2019. 8. p. 226-244.
34. Freeze, R.A. and Cherry, N.J., Groundwater Prentice-Hall Inc. (1979).
35. Subba Rao, N., et al., Geochemical characteristics and controlling factors of chemical composition of groundwater in a part of Guntur district, Andhra Pradesh, India. Environmental earth sciences, 2017. 76. p. 1-22.
36. Selvam, S., et al., Assessment of groundwater from an industrial coastal area of south India for human health risk from consumption and irrigation suitability. Environmental research, 2021. 200. p. 111461.
37. DoE (Department of Environment), The environment conservation rules (E.C.R), government of the people's republic of Bangladesh, Schedule-3, standards for drinking water. Ministry of Environment and Forest, Bangladesh, 1997. p.205–207.
38. World Health Organization (2017) Guidelines for drinking-water quality: first addendum to the fourth edition.
39. Yadav, K.K., et al., GIS-based evaluation of groundwater geochemistry and statistical determination of the fate of contaminants in shallow aquifers from different functional areas of Agra city, India: levels and spatial distributions. RSC advances, 2018. 8(29). p. 15876-15889.
40. Selvam, S., et al., Identification of groundwater contamination sources in Dindugal district of Tamil Nadu, India using GIS and multivariate statistical analyses. 2016. 9. p. 1-14.
41. Vengosh, A., Salinization and saline environments. Treatise Geochem, 2003. 9. p. 612.
42. Isawi, H., et al., Integrated geochemistry, isotopes, and geostatistical techniques to investigate groundwater sources and salinization origin in the Sharm EL-Shiekh Area, South Sinia, Egypt. Water, Air, & Soil Pollution, 2016. 227. p. 1-23.
43. Todd, J.T., et al., The perception of human growth. Scientific American, 1980. 242(2). p. 132-145.
44. Sawyer, C.N. and McCarty, P.L., Chemistry for sanitary engineers. 1967.
45. Islam, S.D.U., et al., Hydrochemical characteristics and quality assessment of groundwater in Patuakhali district, southern coastal region of Bangladesh. Exposure and health, 2017. 9. p. 43-60.
46. Adimalla, N. and Wu, J., Groundwater quality and associated health risks in a semi-arid region of south India: Implication to sustainable groundwater management. Human and ecological risk assessment: an international jour, 2019. 25(1-2). p. 191-216.
47. Musa, O., et al., Physico-chemical characteristics of surface and groundwater in Obajana and its environs in Kogi state, Central Nigeria. African Journal of Environmental Science and Technology, 2014. 8(9). p. 521-531.
48. Onwuka, O. and Omonona, O., Hydrogeochemical characteristics of coastal aquifers from Port Harcourt, southern Nigeria. Environ Earth Sci 76. 2017.
49. Makni, J., S. Bouri, and Ben Dhia, H., Hydrochemistry and geothermometry of thermal groundwater of

southeastern Tunisia (Gabes region). Arabian Journal of Geosciences, 2013. 6. p. 2673-2683.

50. Gibbs, R. j., Mechanisms controlling world water chemistry. 1970. 170(3962). p. 1088-1090.
51. Rao, K.N. and Latha, P.S., Groundwater quality assessment using water quality index with a special focus on vulnerable tribal region of Eastern Ghats hard rock terrain, Southern India. Arabian Journal of Geosciences, 2019. 12. p. 1-16.
52. Mukherjee, A. and Fryar, A.E., Deeper groundwater chemistry and geochemical modeling of the arsenic affected western Bengal basin, West Bengal, India. Applied Geochemistry, 2008. 23(4). p. 863-894.
53. Elango, L. and Kannan, R., Rock–water interaction and its control on chemical composition of groundwater. Developments in environmental science, 2007. 5. p. 229-243.
54. Sonkamble, S., et al., Appraisal and evolution of hydrochemical processes from proximity basalt and granite areas of Deccan Volcanic Province (DVP) in India. Journal of Hydrology, 2012. 438. p. 181-193.
55. Das, B.K. and Kaur, P.J., Major ion chemistry of Renuka lake and weathering processes, Sirmaur district, Himachal Pradesh, India. Environmental Geology, 2001. 40. p. 908-917.
56. Luo, W., Gao, X., & Zhang, X., Geochemical processes controlling the groundwater chemistry and fluoride contamination in the Yuncheng Basin, China—An area with complex hydrogeochemical conditions. PloS one, (2018). 13(7). P. e0199082.https://doi.org/10.1371/journal. pone.0199082
57. Stallard, R. and Edmond, J.M., Geochemistry of the Amazon: 2. The influence of geology and weathering environment on the dissolved load. Journal of Geophysical Research: Oceans, 1983. 88(C14). p. 9671-9688.
58. Sarin, M., et al., Major ion chemistry of the Ganga-Brahmaputra river system: weathering processes and fluxes to the Bay of Bengal. Geochimica et cosmochimica acta, 1989. 53(5). p. 997-1009.
59. Schoeller, H., Geochemistry of groundwater—an international guide for research and practice. UNESCO Paris. (1967). p. 1–18
60. Bhuiyan, M.A., et al., Evaluation of hazardous metal pollution in irrigation and drinking water systems in the vicinity of a coal mine area of northwestern Bangladesh. Journal of hazardous materials, 2010. 179(1-3). p. 1065-1077.
61. Bhuiyan, M.A.H., et al., Assessment of groundwater quality of Lakshimpur district of Bangladesh using water quality indices, geostatistical methods, and multivariate analysis. Environ Earth Sci, 2016. 75. p. 1-23.
62. Huang, G., et al., Impact of anthropogenic and natural processes on the evolution of groundwater chemistry in a rapidly urbanized coastal area, South China. Science of the Total Environment, 2013. 463. p. 209-221.
63. Nosrati, K. and Van Den Eeckhaut, M., Assessment of groundwater quality using multivariate statistical techniques in Hashtgerd Plain, Iran. Journal of Environmental Earth Science, 2012. 65. p. 331-344.
64. Yidana, S.M., Groundwater classification using multivariate statistical methods: Birimian Basin, Ghana. Journal of Environmental Engineering, 2010. 136(12). p. 1379-1388.
65. Wayland, K.G., et al., Identifying relationships between baseflow geochemistry and land use with synoptic sampling and R-mode factor analysis. Journal of Environmental Quality, 2003. 32(1). p. 180-190.
66. Singh, C.K., et al., Multivariate statistical analysis and geochemical modeling for geochemical assessment of groundwater of Delhi, India. Journal of Geochemical Exploration, 2017. 175. p. 59-71.
67. Bahar, M.M. and Reza, M.S., Hydrochemical characteristics and quality assessment of shallow groundwater in a coastal area of Southwest

Bangladesh. Environ Earth Sci, 2010. 61. p. 1065-1073.

68. Singh, A. K., Tewary, B. K., & Sinha, A., Hydrochemistry and quality assessment of groundwater in part of NOIDA metropolitan city, Uttar Pradesh. Journal of the Geological Society of India, 2011. 78(6), p. 523-540.

How to cite this article:
Dina N.T., Kabir M.Z., Deeba F., Rahman S.H., Rasul M.G., Alam M.F., Sultana S. (2025). Appraisal and Evaluation of Hydrogeochemical Processes in the Aquifer System of the South Eastern Coastal Area of Bangladesh.*Journal of Chemistry and Environment*. 4(1). p. 61-80.